TABLE 2. (CONTINUED)

No.	Position	Cat	Gene symbol	Refseq #	Official full name	Ct	E (%)	R
52	E4	PPR49735A	*Neurod1*	NM_019218	Neurogenic differentiation 1	26.39	91.2%	0.9999
53	E5	PPR43535A	*Nkx2-5*	NM_053651	NK2 transcription factor related, locus 5 (Drosophila)	25.63	110.9%	0.9990
54	E6	PPR57763A	*Nodal*	XM_228285	Nodal homolog (mouse)	23.73	129.3%	0.9990
55	E7	PPR52790A	*Nr2f1*	NM_031130	Nuclear receptor subfamily 2, group F, member 1	24.17	102.4%	1.0000
56	E8	PPR46535A	*Nr2f2*	NM_080778	Nuclear receptor subfamily 2, group F, member 2	23.96	108.0%	0.9997
57	E9	PPR59727A	*Pou5f1*	NM_001009178	POU class 5 homeobox 1	24.17	103.1%	0.9998
58	E10	PPR48805A	*Otx2*	XM_224009	Orthodenticle homolog 2 (Drosophila)	23.55	106.7%	0.9998
59	E11	PPR53060A	*Pax3*	XM_343601	Paired box 3	24.83	128.3%	0.9992
60	E12	PPR06696A	*Pdgfra*	XM_214030	Platelet-derived growth factor receptor, alpha polypeptide	24.25	111.0%	0.9992
61	F1	PPR50830A	*Pdx1*	NM_022852	Pancreatic and duodenal homeobox 1	24.02	108.3%	0.9998
62	F2	PPR57592A	*Pecam1*	NM_031591	Platelet/endothelial cell adhesion molecule 1	23.87	126.2%	0.9980
63	F3	PPR46507A	*Pitx2*	NM_019334	Paired-like homeodomain 2	23.53	118.6%	0.9995
64	F4	PPR06704A	*Ptn*	NM_017066	Pleiotrophin	24.74	106.6%	0.9999
65	F5	PPR61896A	*Zfp42*	XM_224882	Zinc finger protein 42	22.87	109.3%	0.9992
66	F6	PPR53039A	*Runx2*	XM_346016	Runt-related transcription factor 2	24.11	95.7%	0.9996
67	F7	PPR68948A	*LOC686412*	XM_001074001	Similar to sal-like 4 isoform a	25.30	97.3%	0.9998
68	F8	PPR44853A	*Shh*	NM_017221	Sonic hedgehog	26.71	110.5%	0.9998
69	F9	PPR47337A	*Epor*	NM_017002	Erythropoietin receptor	24.22	101.4%	0.9996
70	F10	PPR57227A	*Sox15*	XM_343921	SRY (sex determining region Y)-box 15	24.18	98.6%	0.9999
71	F11	PPR43961A	*Sox17*	XM_232640	SRY (sex determining region Y)-box 17	25.28	102.5%	0.9998
72	F12	PPR47353A	*Sox18*	NM_001024781	SRY (sex determining region Y)-box 18	25.54	116.6%	0.9990
73	G1	PPR60530A	*Sox2*	XM_574919	SRY (sex determining region Y)-box 2	25.34	106.8%	0.9996
74	G2	PPR55616A	*Sox7*	XM_224283	SRY (sex determining region Y)-box 7	24.13	108.3%	0.9991
75	G3	PPR53743A	*Sparc*	NM_012656	Secreted protein, acidic, cysteine-rich (osteonectin)	24.39	100.0%	1.0000
76	G4	PPR44745A	*Stat3*	NM_012747	Signal transducer and activator of transcription 3	24.22	126.5%	0.9980
77	G5	PPR68944A	*RGD1559950*	XM_573971	RGD1559950 similar to STELLA	22.50	101.9%	0.9999
78	G6	PPR49061A	*Tbx2*	XM_220810	T-box 2	26.70	93.6%	0.9997
79	G7	PPR53340A	*Tbx3*	NM_181638	T-box 3	24.09	112.7%	0.9995
80	G8	PPR59824A	*Tbx5*	NM_001009964	T-box 5	25.84	103.3%	0.9993
81	G9	PPR66677A	*Tcl1a*	XM_001068183	T-cell leukemia/lymphoma 1A	24.20	104.9%	1.0000
82	G10	PPR50309A	*Tert*	NM_053423	Telomerase reverse transcriptase	24.25	108.4%	0.9995
83	G11	PPR49669A	*Tubb3*	NM_139254	Tubulin, beta 3	23.83	102.9%	0.9999
84	G12	PPR68393A	*Utf1*	XM_001058894	Undifferentiated embryonic cell transcription factor 1	23.61	101.3%	1.0000
85	H1	PPR42363A	*Rplp1*	NM_001007604	Ribosomal protein, large, P1	23.33	101.9%	1.0000
86	H2	PPR42247A	*Hprt1*	NM_012583	Hypoxanthine phosphoribosyltransferase 1	25.02	108.5%	0.9986
87	H3	PPR53027A	*Rpl13a*	NM_173340	Ribosomal protein L13A	21.42	107.7%	0.9990
88	H4	PPR56603A	*Ldha*	NM_017025	Lactate dehydrogenase A	21.90	119.2%	0.9996
89	H5	PPR06557A	*Gapdh*	NM_017008	Glyceraldehyde-3-phosphate dehydrogenase	16.55	123.3%	0.9995
90	H6	PPR63338A	*RGDC*	U26919	Rat Genomic DNA Contamination	23.73	101.9%	1.0000
91	H7	PPX63340A	*RTC*	SA_00104	Reverse transcription control	21.95	107.2%	1.0000
92	H8	PPX63340A	*RTC*	SA_00104	Reverse transcription control	21.50	102.5%	1.0000
93	H9	PPX63340A	*RTC*	SA_00104	Reverse transcription control	21.44	105.4%	0.9992
94	H10	PPX63339A	*PPC*	SA_00103	Positive PCR control	18.80	110.9%	0.9997
95	H11	PPX63339A	*PPC*	SA_00103	Positive PCR control	18.74	108.6%	0.9997
96	H12	PPX63339A	*PPC*	SA_00103	Positive PCR control	18.70	103.6%	0.9998

Qiagen catalog number: CAPR10083, Plate format: 96×1, Real-time instrument: iQ5.

The genes *Ctnnbl1*, *Pias1*, *Hdac2*, *Myod1*, *Neurod1*, and *Sox18* were found to be good candidates for replacement since they did not discriminate cell types. In contrast, the genes *Nanog*, *Afp*, *Gdf3*, *Stella*, *Oct4*, *Utf1*, *Fgf4*, and *Cer1* were able to differentiate cell lines and conditions (see Supplementary Table S1 and Fig. 4).

Discussion

The ability to rapidly analyze gene expression in rat ESC lines using a focused gene array will facilitate the optimization of medium conditions, the characterization of new ESC lines, and confirm that the ESC lines maintain their

undifferentiated state. Here, we describe such an array and evaluated its utility to discriminate undifferentiated rat ESC lines from differentiated ESCs (e.g., ESCs differentiated to EB for 5 or 10 days), from other cells derived from rat embryos such as TS cells and XEN cells, and from MEFs. This array had good inter-operator reproducibility (shown in Fig. 1) and has good QC/QA tools. This focused array produced rapid and reproducible results in a convenient, inexpensive format. Thus, this array will have broad application for laboratories wishing to characterize or optimize rat ESC culture.

When overall gene expression was analyzed, the gene array could discriminate undifferentiated genuine rat ESCs grown from TS, XEN, or MEFs. When overall gene expression was analyzed, the array discriminated undifferentiated rat ESCs grown in 2i plus LIF from rat ESCs that were differentiated for 10 days to EBs. When the expression of individual genes that are highly expressed by undifferentiated ESCs or genes highly expressed during the first 5 to 10 days of differentiation are explored, the array resolved undifferentiated ESCs from EBs differentiated for 5 or 10 days.

The biology of rat ESCs

Currently, the biological differences between mouse, human, and rat ESCs are not well understood. For example, as shown in Fig. 4, undifferentiated, genuine rat ESCs derived in 2i plus LIF and those derived in 4i medium express *Cdx2* and other genes of the trophoblast lineage such as *Hand1* and *Eomes* [7,8,19]. Previously, Cdx2 protein expression in rat ESCs was demonstrated by immunocytochemistry, so it is unlikely this is a false positive [6]. We also noted that Cdx2 expression appears to be >3-fold higher in genuine rat ESCs maintained in 4i (YPAC) conditions compared with 2i plus LIF conditions (see Fig. 4). In fact, genuine rat ESCs derived and maintained in 4i medium had higher expression of *Cdx2* than TS cells. In contrast to *Cdx2* where the expression levels did not discriminate ESCs and TS cells well, TS cells express *Hand1*, *Fgf4*, and *Eomes* at higher levels than genuine rat ESCs. Despite Cdx2 expression by genuine rat ESCs, the array differentiated XEN and TS cells from ESCs based on the expression of *Nanog*, *Pou5f1*, *Fgf4*, *Sox2*, and others (see Fig. 3C). For example, the expression of *Nanog* was >10,000-fold higher in ESCs than either XEN or TS cells. In summary, the expression of *Nanog*, *Oct4*, and *Fgf4* by ESCs and not by XEN and TS cells together with expression of *Gata4* and *Gata6* by XEN and *Hand1* by TS, distinguish XEN and TS cells from ESCs [7,16,18,26].

Since rat ESCs grown in 2i+LIF or 4i are not as efficient at germline transmission as seen in certain mouse strains, we hypothesize that culture conditions that activate or maintain Cdx2 expression might cause rat ESCs to contribute to extraembryonic tissues. This suggests that rat ESCs may contribute to extraembryonic tissues in addition to the inner cell mass following blastocyst injection. Therefore, culture conditions that decrease *Cdx2* gene expression might increase ESC contribution to the inner cell mass and subsequently increase germline transmission efficiency. Further work is needed to confirm this hypothesis.

Technical considerations

The array has elements for QA and QC including 3 elements each for PPC and RTE controls, and an RGDC element. Using the manufacturer's criteria, in 2 arrays, RGDC was questionable. In each case, the technical replicate did not detect RGDC. To further resolve this finding, RT-PCR was performed using a set of primers for Pbgd (also known as Hmbs) that span an intron. The results were unable to verify RGDC. We speculate that the manufacturer's criteria for evaluation of RGDC may generate false positives at a frequency of ~8%. Regarding QA/QC, we noted a tendency for the RNeasy method of total RNA isolation to produce more uniform results compared to the TRIZOL method (see Fig. 1B). A similar observation was noted in the Troubleshooting section of the user's manual provided by the manufacturer. Therefore, it is recommended that a qPCR Grade RNA Isolation Kit be employed with DNase treatment to maximize reproducibility of array findings.

Limitations of this array

Here, we used an array with 86 unique elements. Therefore, there are limitations in terms of the breadth of gene expression information obtained compared with a more global gene expression such as that previously obtained using the Affymetrix rat expression system whose probe set contains >30,000 elements [26]. In their analysis, Li et al. derived and maintained rat ESC-like cells in a medium containing LIF and GSK inhibitor (note their ESC-like cells were shown to form teratoma and to be alkaline phosphatase-positive; they did not test whether their ESC-like cells were competent to contribute to chimera or germline transmission). It is worth pointing out that some of the known pluripotency genes, such as *Tbx3* and *Stella* (Dppa3) were shown to be expressed at high levels in their analysis [26], as was shown to be expressed here (see Table 2). Also, we noted that the primitive endoderm cells that were derived from their rat ESC-like cells expressed high levels of *Gata6*, *Gata4*, *Sox17*, and *Foxa2* [26], similar to what we demonstrated here for the XEN cells (see Fig. 3C, Supplementary Table S4).

In an overall analysis using all genes on the array, the array did not discriminate undifferentiated rat ESCs from EBs differentiated for 5 days. However, genes that are strongly induced by differentiation, such as *Cer1*, *Afp*, *Actc1*, *Foxa2*, *Gata4*, *Gata6*, *Hand1*, *Sox7*, *Sox17*, and *Pdx1*, or particular genes that are strongly downregulated by differentiation, such as *Gdf3* and *Tcl1a*, distinguish rat ESCs that were differentiated for 5 days to EBs from undifferentiated rat ESCs (see Fig. 3B).

Previous work has indicated that expression of certain genes such as *Nanog*, *Oct4*, or *Stella* [17,27–30], epigenetic or microRNA differences [11,31–35] might enrich germline ESCs from other ESCs. Here, the array did not discriminate undifferentiated rat ESC lines that form chimera from genuine rat ESC lines. In fact, no genes were found to be expressed >10-fold difference between chimera 2i ESCs and germline 2i ESCs (see Fig. 3D). Therefore, the role of Dlk1-Dio3 region [34] or the role of miRNAs such as miR-290 miRNA cluster [36–39] might be targets to investigate in rat ESCs in future work.

Acknowledgments

The authors thank Kristin Whiteside, Joseph Smith, and Drs. Brian Petroff, Jay Vivian, and David Albertini for their

encouragement and assistance with this work. Dr. Dan Marcus and COBRE grant NIH/NCRR P20-RR017686 are thanked for use of the Nanodrop. This work was supported by grants from the Johnson Center for Cancer Research, the National Institutes of Health [NS34160 (M.L.W.) and HD020676 (M.J.S.)], the Kansas Biosciences Authority, the University of Kansas Cancer Center pilot project program 2010, the KSU College of Veterinary Medicine Dean's office, and by the State of Kansas Legislature to the Midwest Institute for Comparative Stem Cell Biology. A portion of this work was supported by the Deffenbaugh Foundation to the Spinal Cord Injury Program at the University of Kansas Medical School. MLW thanks BGW for her lifelong support. Mr. and Mrs. Howard Walker are thanked for their hospitality during the fall of 2010.

Author Disclosure Statement

The authors indicate no potential conflicts of interest.

References

1. Hamra FK. (2010). Gene targeting: enter the rat. Nature 467:161–163.
2. Iannaccone PM and HJ Jacob. (2009). Rats! Dis Model Mech 2:206–210.
3. Buehr M, S Meek, K Blair, J Yang, J Ure, J Silva, R McLay, J Hall, QL Ying and A Smith. (2008). Capture of authentic embryonic stem cells from rat blastocysts. Cell 135: 1287–1298.
4. Li P, C Tong, R Mehrian-Shai, L Jia, N Wu, Y Yan, RE Maxson, EN Schulze, H Song, et al. (2008). Germline competent embryonic stem cells derived from rat blastocysts. Cell 135:1299–1310.
5. Tong C, P Li, NL Wu, Y Yan and QL Ying. (2010). Production of p53 gene knockout rats by homologous recombination in embryonic stem cells. Nature 467:211–213.
6. Hong J, H He and ML Weiss. (2011). Derivation and characterization of embryonic stem cells lines derived from transgenic fischer 344 and dark agouti rats. Stem Cells Dev 21:1571–1586.
7. Ralston A and J Rossant. (2005). Genetic regulation of stem cell origins in the mouse embryo. Clin Genet 68:106–112.
8. Sasaki H. (2010). Mechanisms of trophectoderm fate specification in preimplantation mouse development. Dev Growth Differ 52:263–273.
9. Buehr M, J Nichols, F Stenhouse, P Mountford, CJ Greenhalgh, S Kantachuvesiri, G Brooker, J Mullins and AG Smith. (2003). Rapid loss of Oct-4 and pluripotency in cultured rodent blastocysts and derivative cell lines. Biol Reprod 68:222–229.
10. Kawamata M and T Ochiya. (2010). Generation of genetically modified rats from embryonic stem cells. Proc Natl Acad Sci U S A 107:14223–14228.
11. Aiba K, T Nedorezov, Y Piao, A Nishiyama, R Matoba, LV Sharova, AA Sharov, S Yamanaka, H Niwa and MS Ko. (2009). Defining developmental potency and cell lineage trajectories by expression profiling of differentiating mouse embryonic stem cells. DNA Res 16:73–80.
12. Tanaka TS, T Kunath, WL Kimber, SA Jaradat, CA Stagg, M Usuda, T Yokota, H Niwa, J Rossant and MS Ko. (2002). Gene expression profiling of embryo-derived stem cells reveals candidate genes associated with pluripotency and lineage specificity. Genome Res 12:1921–1928.
13. Chuykin I, I Lapidus, E Popova, L Vilianovich, V Mosienko, N Alenina, B Binas, G Chai, M Bader and A Krivokharchenko. (2010). Characterization of trophoblast and extraembryonic endoderm cell lineages derived from rat preimplantation embryos. PLoS One 5:e9794.
14. Debeb BG, V Galat, J Epple-Farmer, S Iannaccone, WA Woodward, M Bader, P Iannaccone and B Binas. (2009). Isolation of Oct4-expressing extraembryonic endoderm precursor cell lines. PLoS One 4:e7216.
15. Galat V, B Binas, S Iannaccone, LM Postovit, BG Debeb and P Iannaccone. (2009). Developmental potential of rat extraembryonic stem cells. Stem Cells Dev 18:1309–1318.
16. Brons IG, LE Smithers, MW Trotter, P Rugg-Gunn, B Sun, SM Chuva de Sousa Lopes , SK Howlett, A Clarkson, L Ahrlund-Richter, RA Pedersen and L Vallier. (2007). Derivation of pluripotent epiblast stem cells from mammalian embryos. Nature 448:191–195.
17. Hayashi K, SM Lopes, F Tang and MA Surani. (2008). Dynamic equilibrium and heterogeneity of mouse pluripotent stem cells with distinct functional and epigenetic states. Cell Stem Cell 3:391–401.
18. Tesar PJ, JG Chenoweth, FA Brook, TJ Davies, EP Evans, DL Mack, RL Gardner and RD McKay. (2007). New cell lines from mouse epiblast share defining features with human embryonic stem cells. Nature 448:196–199.
19. Asanoma K, MA Rumi, LN Kent, D Chakraborty, SJ Renaud, N Wake, DS Lee, K Kubota and MJ Soares. (2011). FGF4-dependent stem cells derived from rat blastocysts differentiate along the trophoblast lineage. Dev Biol 351:110–119.
20. Tanaka S, T Kunath, AK Hadjantonakis, A Nagy and J Rossant. (1998). Promotion of trophoblast stem cell proliferation by FGF4. Science 282:2072–2075.
21. Soares MJ, KD Schaberg, CS Pinal, SK De, P Bhatia and GK Andrews. (1987). Establishment of a rat placental cell line expressing characteristics of extraembryonic membranes. Dev Biol 124:134–144.
22. Vandesompele J, PK De, F Pattyn, B Poppe, RN Van, PA De and F Speleman. (2002). Accurate normalization of real-time quantitative RT-PCR data by geometric averaging of multiple internal control genes. Genome Biol 3:RESEARCH0034.
23. Andersen CL, JL Jensen and TF Orntoft. (2004). Normalization of real-time quantitative reverse transcription-PCR data: a model-based variance estimation approach to identify genes suited for normalization, applied to bladder and colon cancer data sets. Cancer Res 64:5245–5250.
24. Pfaffl MW, A Tichopad, C Prgomet and TP Neuvians. (2004). Determination of stable housekeeping genes, differentially regulated target genes and sample integrity: BestKeeper—Excel-based tool using pair-wise correlations. Biotechnol Lett 26:509–515.
25. Silver N, S Best, J Jiang and SL Thein. (2006). Selection of housekeeping genes for gene expression studies in human reticulocytes using real-time PCR. BMC Mol Biol 7:33.
26. Li C, Y Yang, J Gu, Y Ma and Y Jin. (2009). Derivation and transcriptional profiling analysis of pluripotent stem cell lines from rat blastocysts. Cell Res 19:173–186.
27. Chambers I, J Silva, D Colby, J Nichols, B Nijmeijer, M Robertson, J Vrana, K Jones, L Grotewold and A Smith. (2007). Nanog safeguards pluripotency and mediates germline development. Nature 450:1230–1234.
28. Tanaka TS, DS Lopez, I Lopez de Silanes, LV Sharova, H Akutsu, T Yoshikawa, H Amano, S Yamanaka, M Gorospe and MS Ko. (2006). Esg1, expressed exclusively in preimplantation embryos, germline, and embryonic stem cells, is a

putative RNA-binding protein with broad RNA targets. Dev Growth Differ 48:381–390.
29. Yeom YI, G Fuhrmann, CE Ovitt, A Brehm, K Ohbo, M Gross, K Hubner and HR Scholer. (1996). Germline regulatory element of Oct-4 specific for the totipotent cycle of embryonal cells. Development 122:881–894.
30. Scholer HR, AK Hatzopoulos, R Balling, N Suzuki and P Gruss. (1989). A family of octamer-specific proteins present during mouse embryogenesis: evidence for germline-specific expression of an Oct factor. EMBO J 8:2543–2550.
31. Bao S, F Tang, X Li, K Hayashi, A Gillich, K Lao and MA Surani. (2009). Epigenetic reversion of post-implantation epiblast to pluripotent embryonic stem cells. Nature 461: 1292–1295.
32. Imamura M, K Miura, K Iwabuchi, T Ichisaka, M Nakagawa, J Lee, M Kanatsu-Shinohara, T Shinohara and S Yamanaka. (2006). Transcriptional repression and DNA hypermethylation of a small set of ES cell marker genes in male germline stem cells. BMC Dev Biol 6:34.
33. Surani MA, G Durcova-Hills, P Hajkova, K Hayashi and WW Tee. (2008). Germ line, stem cells, and epigenetic reprogramming. Cold Spring Harb Symp Quant Biol 73:9–15.
34. Liu L, GZ Luo, W Yang, X Zhao, Q Zheng, Z Lv, W Li, HJ Wu, L Wang, XJ Wang and Q Zhou. (2010). Activation of the imprinted Dlk1-Dio3 region correlates with pluripotency levels of mouse stem cells. J Biol Chem 285:19483–19490.
35. Melton C, RL Judson and R Blelloch. (2010). Opposing microRNA families regulate self-renewal in mouse embryonic stem cells. Nature 463:621–626.
36. Babiarz JE, JG Ruby, Y Wang, DP Bartel and R Blelloch. (2008). Mouse ES cells express endogenous shRNAs, siRNAs, and other Microprocessor-independent, Dicer-dependent small RNAs. Genes Dev 22:2773–2785.
37. Judson RL, JE Babiarz, M Venere and R Blelloch. (2009). Embryonic stem cell-specific microRNAs promote induced pluripotency. Nat Biotechnol 27:459–461.
38. Luningschror P, B Stocker, B Kaltschmidt and C Kaltschmidt. (2012). miR-290 cluster modulates pluripotency by repressing canonical NF-kappaB signaling. Stem Cells 30: 655–664.
39. Pfaff N, T Moritz, T Thum and T Cantz. (2012). miRNAs involved in the generation, maintenance, and differentiation of pluripotent cells. J Mol Med (Berlin) 90:747–752.

Address correspondence to:
Dr. Mark L. Weiss
Department of Anatomy and Physiology
Kansas State University College of Veterinary Medicine
Coles Hall
Room 105
Manhattan, KS 66506

E-mail: mlweiss@ksu.edu

Received for publication May 23, 2012
Accepted after revision August 7, 2012
Prepublished on Liebert Instant Online August 14, 2012

SCIENTIFIC REPORTS

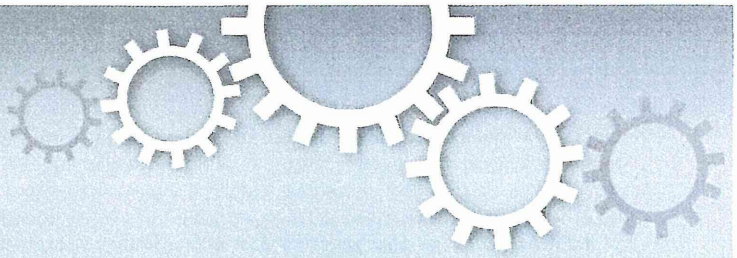

OPEN

SUBJECT AREAS:
PROTEIN DELIVERY
MESENCHYMAL STEM CELLS
MOLECULAR NEUROSCIENCE
PROTEASES

Received
17 October 2012

Accepted
15 January 2013

Published
1 February 2013

Correspondence and requests for materials should be addressed to T.O. (tochiya@ncc.go.jp)

Human adipose tissue-derived mesenchymal stem cells secrete functional neprilysin-bound exosomes

Takeshi Katsuda[1,2], Reiko Tsuchiya[3], Nobuyoshi Kosaka[1], Yusuke Yoshioka[1], Kentaro Takagaki[3], Katsuyuki Oki[3], Fumitaka Takeshita[1], Yasuyuki Sakai[2], Masahiko Kuroda[4] & Takahiro Ochiya[1]

[1]From the Division of Molecular and Cellular Medicine, National Cancer Center Research Institute, 5-1-1 Tsukiji, Chuo-ku, Tokyo 104-0045, Japan, [2]Institute of Industrial Science (IIS), The University of Tokyo, 4-6-1 Komaba, Meguro-ku, Tokyo 153-8505, Japan, [3]Research and Development Dept., SEEMS Inc., 2-4-32 Aomi, Koto-ku, Tokyo 135-0064, Japan, [4]Department of Pathology, Tokyo Medical University, 6-1-1, Shinjuku, Shinjuku-ku, Tokyo, 160-8402, Japan.

Alzheimer's disease (AD) is characterized by the accumulation of β-amyloid peptide (Aβ) in the brain because of an imbalance between Aβ production and clearance. Neprilysin (NEP) is the most important Aβ-degrading enzyme in the brain. Thus, researchers have explored virus-mediated NEP gene delivery. However, such strategies may entail unexpected risks, and thus exploration of a new possibility for NEP delivery is also required. Here, we show that human adipose tissue-derived mesenchymal stem cells (ADSCs) secrete exosomes carrying enzymatically active NEP. The NEP-specific activity level of 1 μg protein from ADSC-derived exosomes was equivalent to that of ~ 0.3 ng of recombinant human NEP. Of note, ADSC-derived exosomes were transferred into N2a cells, and were suggested to decrease both secreted and intracellular Aβ levels in the N2a cells. Importantly, these characteristics were more pronounced in ADSCs than bone marrow-derived mesenchymal stem cells, suggesting the therapeutic relevance of ADSC-derived exosomes for AD.

Alzheimer's disease (AD) is a progressive and fatal neurodegenerative disorder that is characterized by memory loss and cognitive ability deterioration. The accumulation of β-amyloid peptide (Aβ) in the brain plays a critical role in AD pathogenesis[1,2]. The steady-state level of Aβ is determined by a balance between its biosynthesis and clearance[3]. The physiological metabolite Aβ is constantly produced and removed in the brain, and it has been demonstrated that even small decreases in its removal lead to Aβ deposition[3]. Among several proteases involved in the proteolysis of Aβ, neprilysin (neutral endopeptidase: NEP), a type II membrane-associated metalloendopeptidase, appears to be the most important[4,5]. Indeed, AD patients show decreased expression and activity of NEP[6]. Thus, NEP has been intensively studied as a potential therapeutic target for AD[7]. One promising approach for lowering brain Aβ levels is the delivery of NEP. Recent reports have indicated that NEP gene delivery either peripherally or within the brain is effective in clearing brain Aβ[7]. However, safety issues related to the use of viral vectors limit the feasibility of this approach.

NEP, more often referred to as CD10, is expressed by mesenchymal stem cells (MSCs)[8,9]. However, to our knowledge, no study has explored the therapeutic potential of MSCs with regard to their Aβ degrading capacity. MSCs initially attracted interest for their ability to differentiate into cells of mesodermal lineage *in vitro* and *in vivo*[11]. Furthermore, in the last decade, it has been demonstrated that MSCs have many other functional properties. They can differentiate into cells from unrelated germline lineages, resist immunosurveillance, home to injured tissue, and secrete factors with immunosuppressive, anti-apoptotic, and trophic effects[10,11]. Accordingly, there is growing evidence that MSC-based therapies could benefit a wide range of neurodegenerative diseases[12], including AD[13–18]. The mechanisms by which transplanted MSCs influence AD have been roughly classified as cellular replacement[13,14] or paracrine secretion[15–18], but the precise mechanism remains unclear. Thus, any possible mechanism of AD pathophysiology should be investigated, and any possible strategy for AD treatment should be explored.

Another recently reported remarkable feature of MSCs is their ability to secrete exosomes with therapeutic potential[19]. Exosomes are small, intraluminal vesicles of multivesicular bodies released when they fuse with the plasma membrane[20]. It has been suggested that these vesicles are produced by a variety of cell types and can function as intercellular transmitters of mRNA, microRNA, and proteins[21–23]. The first evidence of the

therapeutic potential of MSC-derived exosomes was in a mouse model of acute kidney injury[24]. Bruno et al. found that bone marrow-derived (BM−) MSC exosomes activated a proliferative program in surviving tubular cells after injury via a horizontal transfer of mRNA. Lai et al. also reported that MSC-derived exosomes exerted therapeutic effects on myocardial ischemia/reperfusion injury[25].

Given that exosomes are membrane vesicles and that MSCs express membrane-bound enzyme NEP, it can be assumed that MSCs would secrete exosomes with NEP on their membrane. Here, we report for the first time that adipose tissue-derived MSCs (ADSCs) produce NEP-bound exosomes approximately 100–200 nm in diameter. Furthermore, co-culture of N2a cells overproducing human Aβ with ADSCs led to decreases in the secreted Aβ40 and 42 levels as well as a decrease in the intracellular Aβ42 level. Importantly, these characteristics were more pronounced in ADSCs than BM-MSCs, suggesting the therapeutic relevance of ADSC-derived exosomes for AD.

Results

ADSCs express NEP at a higher level than BM-MSCs. To select the optimal source of MSCs for the present study, we performed comparative analyses on NEP expression between ADSCs and BM-MSCs. A flow cytometry analysis indicated that NEP-positive populations in ADSCs were greater than those in BM-MSCs (Fig. 1A); regarding the other surface markers, they showed the similar profiles that are characteristic to MSCs (positive for CD105, CD73, CD90, and CD44; negative for CD45, CD31, and CD34) (Fig. S1). By qRT-PCR analysis, we confirmed that NEP gene expression levels were considerably higher in ADSCs from each donor than in BM-MSCs from all 4 donors (Fig. 1B). In addition, immunoblot analysis revealed that the NEP protein expression level in ADSCs was ~ 4-fold higher than that of BM-MSCs (Fig. 1C). This observation was further confirmed by immunocytochemistry, where ADSCs were stained for NEP more strongly than BM-MSCs (Fig. 1D). Collectively, these results demonstrate that ADSCs express more NEP than BM-MSCs. Thus, we mainly focused on ADSCs for the subsequent experiments.

ADSC-derived NEP exhibits specific enzyme activity. To investigate the feasibility of using ADSC-derived NEP as a therapeutic target, we examined whether ADSCs indeed exhibited NEP-specific enzyme activity. We measured NEP-specific enzyme activity using a fluorogenic peptide substrate, Mca-RPPGFSAFK(Dnp), and a selective NEP inhibitor, thiorphan. This substrate can be cleaved by several endopeptidases, including NEP, endothelin-converting enzyme (ECE)-1, ECE-2, angiotensin-converting enzyme (ACE)-1, ACE-2, and insulin-degrading enzyme (IDE)[26]. However, at pH 7.5, the use of thiorphan allows the discrimination of NEP enzyme activity from other closely related enzymes[26].

Cell lysates of ADSCs from each donor exhibited enzyme activity both in the presence and absence of thiorphan (Figs. S2 A-D). NEP-specific activity, calculated after the subtraction of fluorescence in the presence of thiorphan, demonstrated that all ADSCs exhibited NEP-specific enzyme activity (Fig. 2A). NEP-specific enzyme activity accounted for 38.3 ± 4.5% of total enzyme activity (Fig. 2B), and the activity level of 1 μg ADSC cell lysate was estimated to be equivalent to that of 0.35 ± 0.14 ng recombinant human NEP (rhNEP) (Fig. 2C, termed as NEP activity index). In contrast to the above observation, BM-MSCs showed weak or undetectable NEP enzyme activity (Fig. 2D). Intriguingly, the total enzyme activity of BM-MSCs measured in the absence of thiorphan was comparable to that of ADSCs (Figs. S3 A, B). That is, NEP-specific enzyme activity contributed relatively little to the total enzyme activity of BM-MSCs (Fig. 2D), suggesting that NEP activity is a unique characteristic of ADSCs. These results support the idea that NEP expressed by ADSCs, but not BM-MSCs, may be therapeutically useful for AD.

ADSCs secrete exosomes to their culture supernatant. Recently, it has been shown that exosomes secreted by MSCs contribute to their paracrine effects[19,25,26]. Considering the reports that transplanted MSCs influenced AD via their paracrine effects[15–18], we hypothesized that ADSC-derived exosomes would have therapeutic potential for AD, especially by focusing on their NEP producing ability.

To test whether ADSCs could secrete NEP via exosome release, we isolated putative exosome fractions from conditioned media of ADSCs from 4 donors (#1–4) with a standard ultracentrifugation method[27,28]. The phase-contrast electron micrographs of the exosomes revealed rounded and double-membraned structures with a size of approximately 60–200 nm (Fig. 3A). Immunoblot analyses revealed that tetraspanin CD81, a reliable exosomal marker[29], was present in the exosome fraction but absent in the donor cell lysates (Fig. 3B). We also confirmed the presence of CD63, another well-established exosome marker[29] (Fig. 3B). CD63 was also detected in the cell lysate, but this is in accordance with the fact that CD63 is expressed by MSCs[30]. In contrast, cellular proteins cytochrome c and actin were detected exclusively in the cell lysates (Fig. 3B). Then, we analyzed the size distribution of the isolated exosomes by two distinct methods: NTA and scanning ion occlusion sensing (SIOS). The size distribution was physically homogeneous with a peak at 150–200 nm, as determined by nanoparticle tracking analysis (NTA) (Fig. 3C, E), or at 110–160 nm, as determined by SIOS (Fig. 3D, E). The size of ADSC-derived exosomes was relatively larger than that of previously reported exosomes, which were 50–100 nm in diameter. The exosome yield per 10^6 ADSCs per day was 1–4 × 10^8 particles, as determined by NTA, or 1–4 μg protein, as determined by the Bradford method (Fig. 3E). Collectively, these results reveal that ADSCs secrete exosomes to the culture supernatant.

ADSC-derived exosomes contain enzymatically active NEP. It is thought that the molecular composition of exosomes reflects the specialized functions of their original cells[19,31]. Thus, we next asked whether ADSC-derived exosomes contained enzymatically active NEP. Immunoblot analyses revealed that exosomes secreted by each line of donor-derived ADSCs contained NEP (Fig. 4A). Of note, the enzyme activity assay using a fluorogenic substrate revealed that these exosomes exhibited NEP-specific activity (Fig. 4B). Interestingly, comparison of exosomal enzyme activity in the presence and absence of thiorphan demonstrated that NEP-specific activity accounted for a large proportion of the total activity (Fig. 4C, D): the enzyme activity was almost completely lost in the presence of thiorphan (Fig. 4D). The NEP-specific activity / total activity ratios of ADSC-derived exosomes reached 89.5 ± 4.4% (Fig. 4E). NEP-specific activity level of 1 μg protein from ADSC-derived exosomes was estimated to be equivalent to 0.26 ± 0.07 ng rhNEP (Fig. 4F, Fig. 4S). In addition, we confirmed that ADSC-derived exosomes exhibited a higher NEP-specific activity than BM-MSC-derived esosomes (Fig. 4G). These results demonstrate that ADSC-derived exosomes possess enzymatically active NEP, implying that they can serve as a novel NEP protein delivery system.

ADSCs decrease both the extracellular and intracellular Aβ levels of N2a cells. To test whether ADSCs could contribute to decrease of both synthesized and secreted Aβ, we co-cultured ADSCs or BM-MSCs with a neuroblastoma cell line N2a cells genetically modified to overproduce human Aβ (Fig. 5A)[32]. Both Aβ40 and 42 levels in the N2a cell culture media were significantly decreased after co-culture with ADSCs or BM-MSCs (Fig. 5B, C). The decreasing degrees of both secreted Aβ40 and 42 levels were greater in co-culture with ADSCs than BM-MSCs (Fig. 5B, C). Of note, we also found that

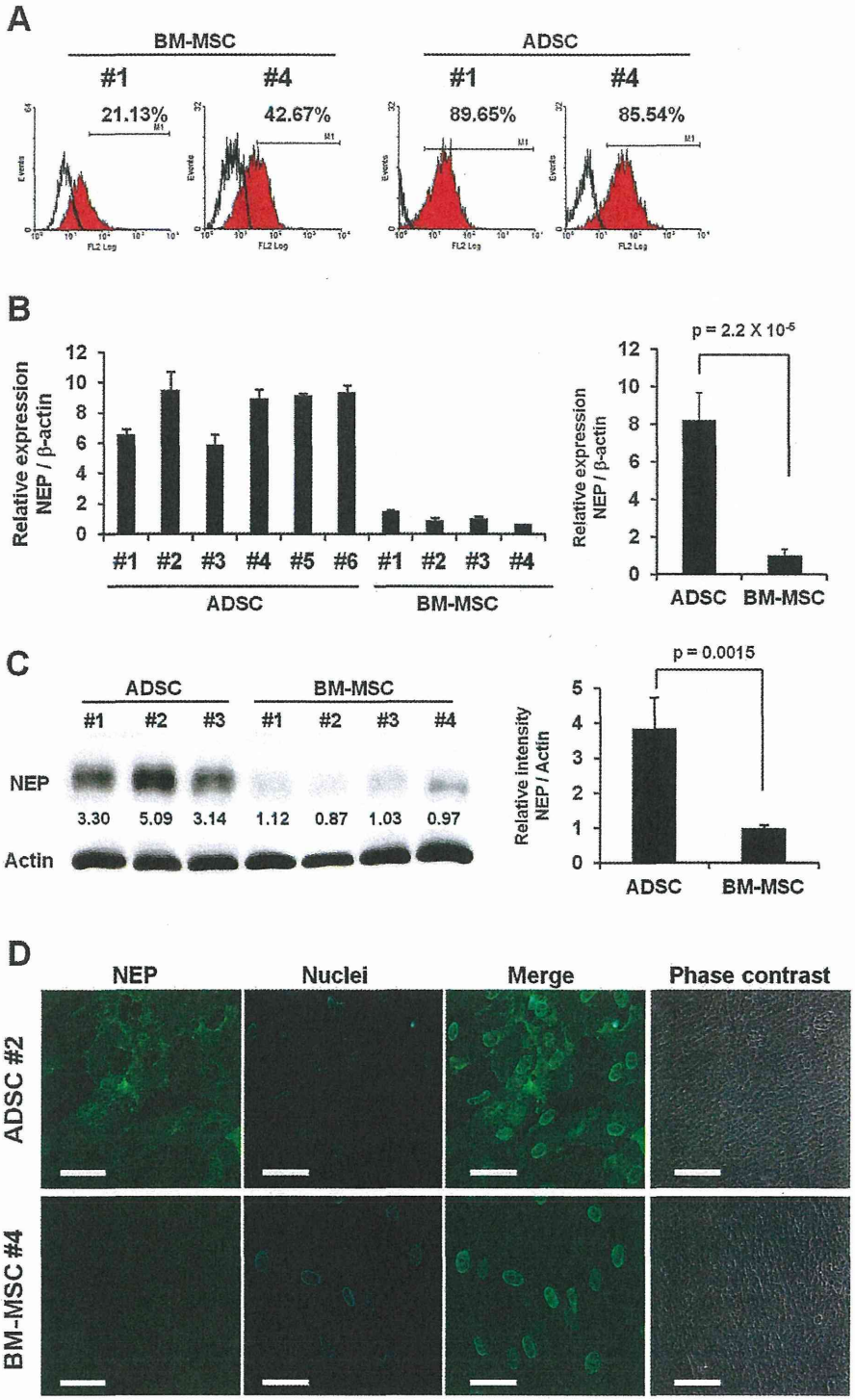

Figure 1 | ADSCs express NEP at a higher level than BM-MSCs. (A) Flow cytometry results of ADSCs #1 and #4 and BM-MSCs #1 and #4 for NEP. (B) qRT-PCR analysis of NEP in ADSCs and BM-MSCs. Transcript levels were normalized to β-actin levels. Data are the mean ± S.D. (n = 3). (C) Cell lysates of ADSCs or BM-MSCs were analyzed by immunoblotting with an anti-NEP or an anti-actin antibody (left). Either 3 μg or 1 μg of cell lysate protein per lane was loaded for NEP and actin, respectively. The relative signal intensity (NEP/Actin) for each sample was measured, and normalized values are shown in the graph. The average values of ADSCs and BM-MSCs are compared on the right. Data are the mean ± S.D. (D) Immuno cytochemistry of ADSCs for NEP. ADSCs were stained with a mouse-anti NEP monoclonal antibody (green), and nuclei were counterstained with Hoechst 33342 (blue). Scale bar: 50 μm.

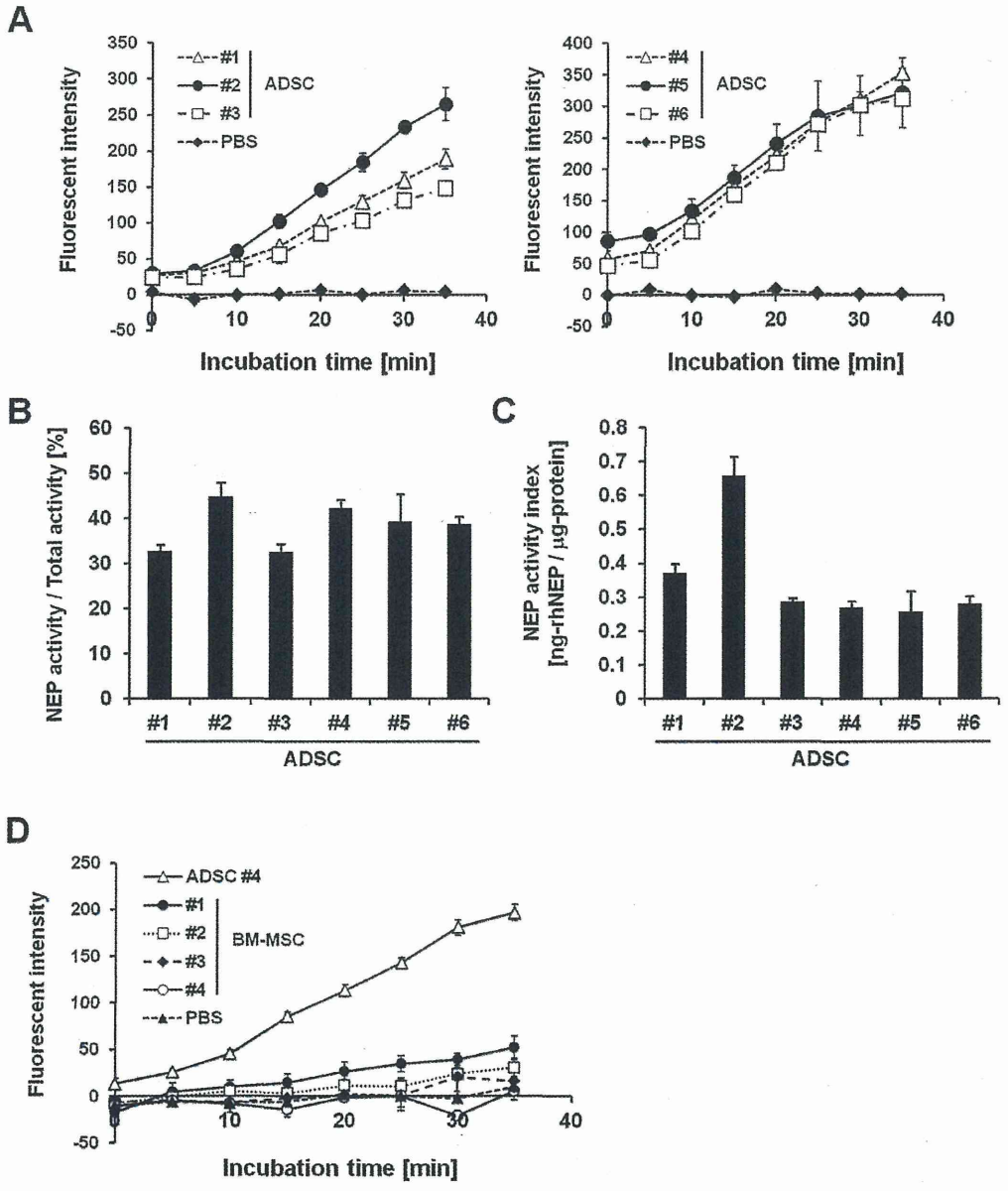

Figure 2 | ADSCs, but not BM-MSCs, exhibit NEP-specific enzyme activity. (A) NEP-specific enzyme activity was measured in ADSC cell lysates (left: #1–3 and right: #4–6) using a fluorogenic peptide substrate, Mca-RPPGFSAFK(Dnp). The average NEP activity represented by fluorescence intensity was measured with a reading interval of 5 min. The specific NEP activity was calculated by subtracting residual fluorescent intensity after incubation with the NEP inhibitor thiorphan (Fig. S2 A–D). Data are the mean ± S.D. (n = 3). (B) NEP contribution ratio calculated as the percentage ratio of NEP-specific activity rate to total activity rate. NEP-specific or total enzyme activity rate was determined as the gradient of the corresponding time course of fluorescent intensity. Data are the mean ± S.D. (n = 3). (C) NEP-specific enzyme activity levels of ADSCs were estimated from rhNEP standard curves (Fig. S2 E–H) and represented as the value ng-rhNEP/μg-protein (termed as NEP activity index in the diagram). Data are the mean ± S.D. (n = 3). (D) Comparison of NEP-specific enzyme activity levels between ADSC #4 and BM-MSCs #1–4. Data are the mean ± S.D. (n = 3).

the intracellular Aβ42 level in N2a cells was significantly decreased by co-culture with ADSCs or BM-MSCs (Fig. 5D). This suggests that NEP-loaded exosomes secreted by ADSCs or BM-MSCs entered the cytoplasm of N2a cells, and degraded the intracellular Aβ of N2a cells. Indeed, addition of thiorphan raised the intracellular Aβ42 level from 77% to 92% of that of the control (Fig. 5E). We also confirmed that ADSC-derived exosomes, at least in part, contributed to decreasing the intracellular Aβ42 level in N2a cells (Fig. S5).

ADSC-derived exosomes are incorporated into neuroblastoma cells. To verify that ADSC transferred their exosomes to N2a cells, we co-cultured PKH26 labeled ADSCs with PKH67 labled N2a cells (Fig. 6A). One day after co-culture, some, but not all, N2a cells were co-stained with PKH26 and PKH67, suggesting that exosomes secreted by ADSCs were transferred to N2a cells (Fig. 6A). Interestingly, however, we did not observe co-stained ADSCs, suggesting a certain mechanism underlying the unidirectional transport of exosomes from ADSCs to N2a cells, but not from N2a cells to ADSCs. Exosomal membrane is rich in ceramide, which may lead to inefficient incorporation of the cell membrane-linked PKH into the secreted exosomes[33]. Thus, we next directly labeled ADSC-derived exosomes with PKH67, and examined whether these

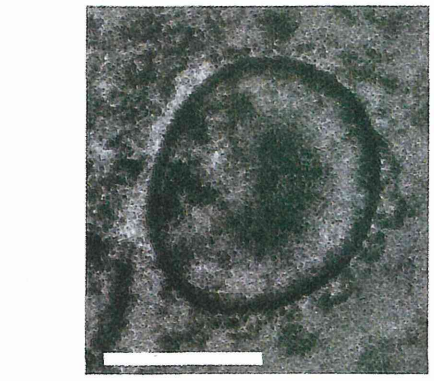

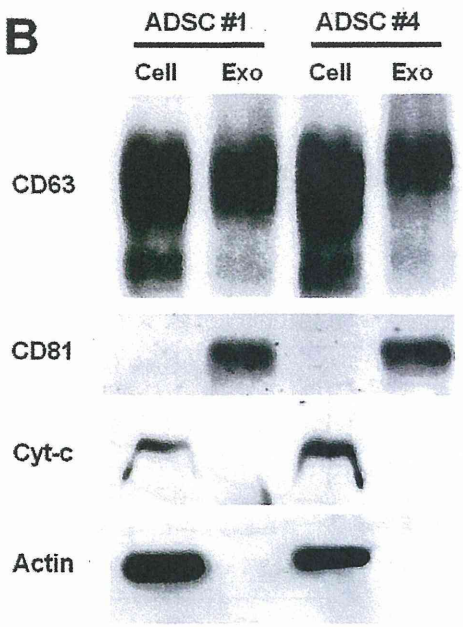

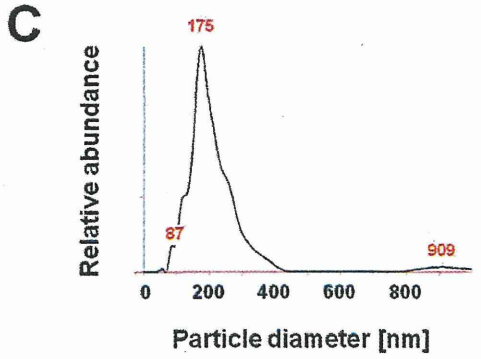

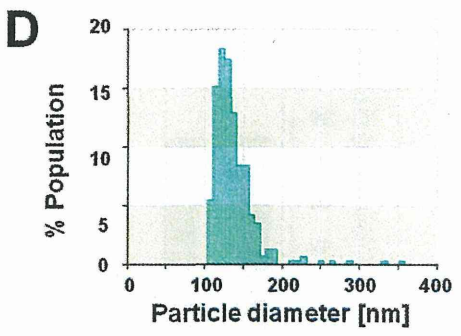

E

		Yield [/ 10^6 cells / d]		Peak diameter [nm]	
		Protein [μg]	X 10^8 Particles	By NTA	By SIOS
ADSC	#1	3.5 ± 1.6	3.2 ± 1.6	175	118.9
	#2	2.8 ± 1.5	1.4 ± 0.26	169	127.8
	#3	1.7 ± 0.55	1.6 ± 0.56	136	—
	#4	3.8 ± 1.1	—	160	117.3

Figure 3 | ADSCs secrete 100–200 nm exosomes. (A) A phase-contrast transmission electron micrograph of purified ADSC #4-derived exosomes. Scale bar: 100 nm. (B) The exosome fractions and cell lysates of ADSCs #1 and #4 were analyzed by immunoblotting with antibodies against exosomal proteins CD63 and CD81 and cellular proteins cytochrome-c (Cyt-c) and actin (CD63 under nonreducing conditions). Equal amounts of protein from cell lysates or exosomes were used for each assay: 0.5 μg for CD63, 5 μg for CD81 and Cyt-c, and 1 μg for actin. (C, D) Size distribution of ADSC#1-derived exosomes as measured by nanoparticle tracking analysis (NTA) showed a peak at 175 nm (C), and scanning ion occlusion sensing (SIOS) showed a peak at 118.9 nm (D). (E) Yields and peak diameters of exosomes produced by ADSCs #1–4 are summarized. Protein amounts and particle numbers of harvested exosomes were determined by the Bradford method and NTA, respectively. Peak diameters were determined by NTA and SIOS. Data are the mean ± S.D. (n = 3–4).

exosomes were incorporated into N2a cells (Fig. 6B). Seven hr after exosome addition to N2a culture medium, some of the cells were already stained green. Furthermore, after 24 hr, most N2a cells were stained green, indicating that ADSC-derived exosomes were efficiently transferred into recipient N2a cells. Collectively, it was demonstrated that ADSCs transferred their exosomes to N2a cells, which may lead to the decrease in the intracellular Aβ42 level of N2a cells.

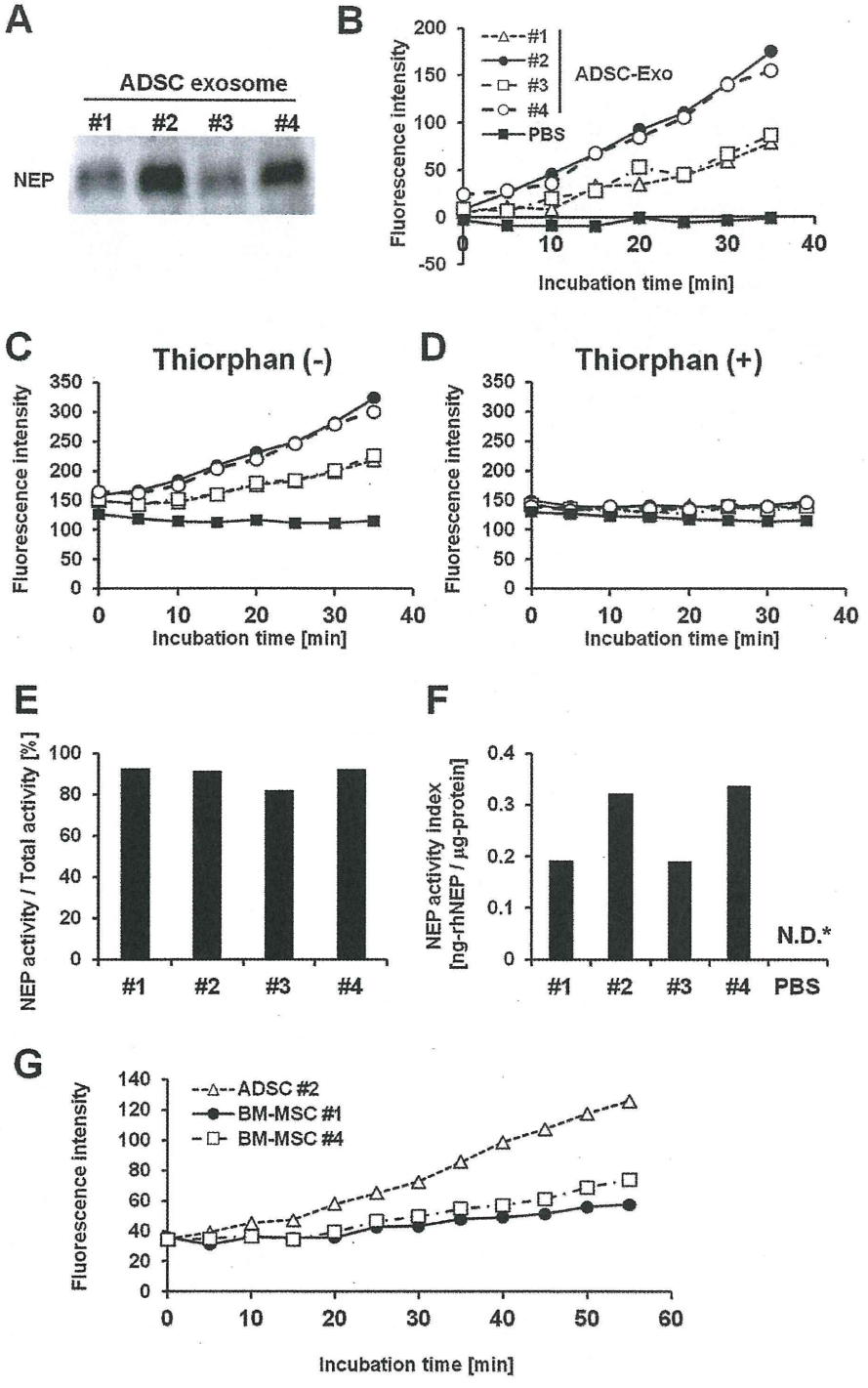

Figure 4 | ADSC-derived exosomes possess enzymatically active NEP. (A) Immunoblotting for NEP of exosomes isolated from ADSCs #1–4. (B–D) NEP enzyme activity assay for ADSC-derived exosomes (#1–4). NEP enzyme activity was measured using a fluorogenic peptide substrate, Mca-RPPGFSAFK(Dnp) and NEP inhibitor thiorphan. NEP specific activity (B) was calculated by subtracting the residual fluorescence intensity measured in the presence of thiorphan (D) from the total enzyme activity measured in the absence of thiorphan (C). Addition of thiorphan sharply reduced the enzyme activity of ADSC-derived exosomes (D). (E) NEP contribution ratio for ADSC-derived exosomes calculated as the percentage ratio of NEP-specific activity rate to total activity rate. (F) NEP-specific enzyme activity levels of exosome fractions of ADSCs #1–4 were estimated from a rhNEP standard curve (Fig. 4S) and are represented as the value ng-rhNEP/µg protein (termed as NEP activity index in the diagram). N.D. indicates "not determined".